





Article

Gas-Supported Triboelectric Nanogenerator Based on In Situ Gap-Generation Method for Biomechanical Energy Harvesting and Wearable Motion Monitoring

Changjun Jia ¹, Yongsheng Zhu ¹, Fengxin Sun ¹, Yuzhang Wen ¹, Qi Wang ², Ying Li ³, Yupeng Mao ^{1,4,*} and Chongle Zhao ^{1,*}

¹ Physical Education Department, Northeastern University, Shenyang 110819, China

² College of Sciences, Northeastern University, Shenyang 110819, China

³ Art College, Liaoning Communication College, Shenyang 110136, China

⁴ School of Strength and Conditioning Training, Beijing Sport University, Beijing 100084, China

* Correspondence: maoyupeng@pe.neu.edu.cn (Y.M.); zhaochongle@pe.neu.edu.cn (C.Z.)

Abstract: The rapid development of wearable electronic devices (such as in applications for health care monitoring, intelligent sports, and human–computer interaction) has led to a huge demand for sustainable energy. However, the existing equipment cannot meet the requirements of energy harvesting, wearable sensing, and environmental protection concurrently. Herein, by an environmentally friendly in situ gap-generation method and doping technology, we have manufactured an Ecoflex–PVDF composite material as a negative triboelectric layer and used gas as a support layer for the triboelectric nanogenerator (EPGS-TENG). The device has excellent electrical output performance and working stability (pressure sensitivity of 7.57 V/N, angle response capacity of 374%, output power of 121 μ W, temperature adaptability from 20 °C to 40 °C, durability over 3 h, and stability of 10 days). EPGS-TENG can meet the requirements of biomechanical energy collection and wearable self-powered sensing simultaneously. EPGS-TENG shows great application potential for the new generation of wearable devices.

Keywords: triboelectric nanogenerator; sustainable energy harvesting; wearable motion sensing



Citation: Jia, C.; Zhu, Y.; Sun, F.; Wen, Y.; Wang, Q.; Li, Y.; Mao, Y.; Zhao, C. Gas-Supported Triboelectric Nanogenerator Based on In Situ Gap-Generation Method for Biomechanical Energy Harvesting and Wearable Motion Monitoring. *Sustainability* **2022**, *14*, 14422. <https://doi.org/10.3390/su142114422>

Academic Editor: Changhyun Roh

Received: 6 September 2022

Accepted: 31 October 2022

Published: 3 November 2022

Publisher's Note: MDPI stays neutral with regard to jurisdictional claims in published maps and institutional affiliations.



Copyright: © 2022 by the authors. Licensee MDPI, Basel, Switzerland. This article is an open access article distributed under the terms and conditions of the Creative Commons Attribution (CC BY) license (<https://creativecommons.org/licenses/by/4.0/>).

1. Introduction

With the remarkable progress of the Internet of Things and artificial intelligence, wearable electronic devices have developed rapidly in the past few years. They have attracted significant research interest in many fields such as medical monitoring [1–3], intelligent movement [4–6], and human–computer interaction [7–9]. However, rapid development faces a critical challenge. Most wearable electronic devices are powered by external batteries, which have a short life span, difficulty in replacement, and energy pollution [10–12]. A very promising solution is to effectively convert renewable energy in the environment into electric energy to supply power for these devices. For this reason, researchers have invested significant effort into solving the energy supply problems of wearable devices, such as through solar cells [13,14], thermoelectric generators [15,16], and piezoelectric nanogenerators [17,18]. However, because of the cost, manufacturing process, material selection, and energy conversion efficiency, its large-scale practical application is limited. The triboelectric nanogenerator (TENG), invented by Zhonglin Wang, is a new potential energy conversion technology. TENG can transform neglected and widespread mechanical energy into electrical energy, which makes it possible to collect biological mechanical energy [19–30] and self-powered sensing [31–36].

The triboelectric nanogenerator (TENG) is based on coupling, the contact charge effect, and the electrostatic induction effect [37,38]. It has the advantages of simple manufacture, a wide selection of materials, diverse working modes, and excellent flexibility [39–43].

TENG can not only be used as a self-powered sensor to monitor various mechanical stimuli in the surrounding environment but can also be used as an energy harvester to convert low-frequency and irregular mechanical energy into electrical energy. However, most TENGs need an auxiliary gasket as supporting layer [23,34,40,44–47]. On the one hand, these gaskets easily fall off, which can prevent TENG from working; on the other hand, the dropped auxiliary gasket will also cause environmental pollution. Danna Zhao et al. innovatively demonstrated an eco-friendly in situ gap-generation method to fabricate a no-spacer triboelectric nanogenerator (NSTENG) for monitoring cardiovascular activities. The TENG made by this method has a good motion perception ability, and the equipment made by this method has good biocompatibility and environmental safety [48]. However, the device manufactured by this method has low electrical output capacity, and cannot be used as an energy harvester. The electrical output performance of TENGs is mainly determined by the induced surface charge density and charge trapping ability of triboelectric materials [49,50]. Although silicone rubber is the first choice for the triboelectric layer because of its high electronegativity, flexibility, and easy processing [51,52], its performance is still insufficient to meet the actual demand. The TENG performance of silica gel can be further improved by reasonable preparation, such as doping [53,54] and surface modification [55,56].

Herein, we designed an EPGS-TENG. We used an Ecoflex–PVDF composite material as the EPGS-TENG negative triboelectric layer and gas as a supporting layer. The gas support layer can be generated in situ by evaporating deionized water soaked on the copper electrode. The output performance of the TENG can be improved by doping PVDF, so that the EPGS-TENG can simultaneously serve both biomechanical energy harvesting and wearable self-powered sensing. The EPGS-TENG has good sensory sensitivity, electrical output performance, and working stability: with pressure sensitivity of 7.57 V/N, angle response capability of 374%, output voltage 13 times higher than that of undoped TENG, an output power of 121 μ W, stability from 20 °C to 40 °C, and durability over 3 h. EPGS-TENG can be used as an energy harvester to collect biomechanical energy and provide power for commercial electronic products without an additional power supply. In addition, EPGS-TENG can be used as a wearable self-powered sensor, which can be attached on different joints of the human body to monitor movement. By constructing the wireless transmission system of EPGS-TENG, human motion information can be displayed in real time with a computer terminal. In the new round of scientific and technological revolution and industrial transformation, the EPGS-TENG can be seen as a booster to accelerate the digitalization and intelligence of sports.

2. Materials and Methods

2.1. Materials

Smooth-on Ecoflex 00-30 was purchased from Beijing Lancheng Feifan Technology Co., Ltd. (Beijing, China). Polyvinylidene fluoride (PVDF) powder with a particle size of 10–20 μ m was purchased from Suzhou Qingxu Plasti-cizing Co., Ltd. (Suzhou, China). Enameled wire was purchased from Wuhu Eriter Electromechanical Equipment Co., Ltd. (Wuhu, China). The one-sided matte copper foil was purchased from Taizhou Beiling Strength Store (Taizhou, China).

2.2. Preparation of Ecoflex–PVDF Mixed Glue Solution

The manufacturing process is as follows: (1) Weigh 0.12 g PVDF powder. (2) The PVDF powder is poured into 4 g of Eco flex A glue solution and stirred for 15 min. (3) A measure of 4 g of Ecoflex B glue solution is added to the above mixed glue solution and stirred for 30 min. Ensure that PVDF nanoparticles are evenly mixed in Ecoflex glue solution. (4) The mixed glue is shaken by an ultrasound for 5 min and left standing for 10 min. A mixture without bubbles is obtained.

2.3. Fabrication of the EPGs-TENG

(1) Preparation of casting mold: The 5 cm × 3 cm × 0.5 cm acrylic sheet is cut out into a 3 cm × 2.5 cm × 0.25 mm pit by a laser cutting machine (100 W off-line high matching). (2) The Ecoflex–PVDF mixed glue solution is poured into the mold, and then the mold is moved to a 35 °C oven. When the glue solution is completely cured, a 3 cm × 2.5 cm Ecoflex–PVDF mixture substrate is formed. (3) The copper foil is cut to a size of 2.5 cm × 2 cm and placed on the mixture substrate with the matte side facing up. Then, the surface of the copper foil is soaked with 2 μL of deionized water. Note that, because the copper foil is coarsened, it has good hydrophilicity. Water droplets on the copper foil are not only evenly distributed, but they also reduce the overall thickness of EPGs-TENG. The enameled wire is connected to the back of the copper foil as a connecting wire. (4) Pour the Ecoflex–PVDF mixed glue solution into the mold again, so that the glue solution completely seals the deionized water and the copper foil. After standing for 12 h (at room temperature), take the device out of the mold. (5) Finally, the device is transferred to an oven and heated at 100 °C for 5 h, so that the deionized water in the device completely changes into water vapor.

2.4. Characterization and Measurements

The fabricated EPGs-TENG is fixed on the acrylic fixing frame opposite the stepper motor with adhesive tape. The linear motor is set to output motions of different amplitudes and frequencies, simulating human joint motion through the control system. The EPGs-TENG generates a triboelectric signal by a linear motor that hits repeatedly and periodically. An oscilloscope (sto1102c, Shenzhen, China) is used to collect the electrical signals generated by TENG, which is attached to the body or stepping motor.

3. Results and Discussion

Figure 1a shows a schematic illustration of the application of EPGs-TENG as a new-generation wearable device. EPGs-TENG can be attached to the joints of the human body to collect biomechanical energy generated during movement. In addition, EPGs-TENG can be used as a self-powered sensor to accurately monitor human motion information. EPGs-TENG adopts a single-electrode structure, which is composed of a copper electrode and an Ecoflex–PVDF composite triboelectric layer on the outside, in which the inside is supported by evaporated water vapor. The manufacturing process of EPGs-TENG is shown in Figure 1b. EPGs-TENG can be manufactured by a simple process. The detailed manufacturing process can be found in the Materials and Methods section. Firstly, the PVDF powder is poured into the Ecoflex-A glue solution, and then it is stirred to obtain the Ecoflex-A-PVDF mixed glue solution. Secondly, the Ecoflex-B glue is poured into the mixed glue, and the homogenized Ecoflex–PVDF glue is obtained after being stirred fully. Thirdly, the copper electrode with deionized water on the surface is sealed in the acrylic mold with the Ecoflex–PVDF mixed glue solution. Finally, after the Ecoflex–PVDF mixed glue solution is cured, the device is transferred to 100 °C for heating, so that the deionized water on the copper surface evaporates, and a gas support layer forms in situ. Figure 1c,d show the optical photos of EPGs-TENG in the original state and the bent state, respectively, which shows that it has excellent flexibility, and can fit well with human joints. The gas layer supporting the EPGs-TENG can be clearly observed in Movie S1. The cross-sectional view of EPGs-TENG is shown in Figure S1. The proposed highly negative Ecoflex–PVDF can be combined with positive copper electrodes to form high-performance TENGs, as shown in the energy band diagram in Figure 1e. The triboelectric charge density of the Ecoflex–PVDF layer is affected by PVDF. The addition of PVDF nanoparticles can improve the ability of the negative triboelectric layer to capture, charge, and increase the surface potential difference between the triboelectric layer and the copper electrode.

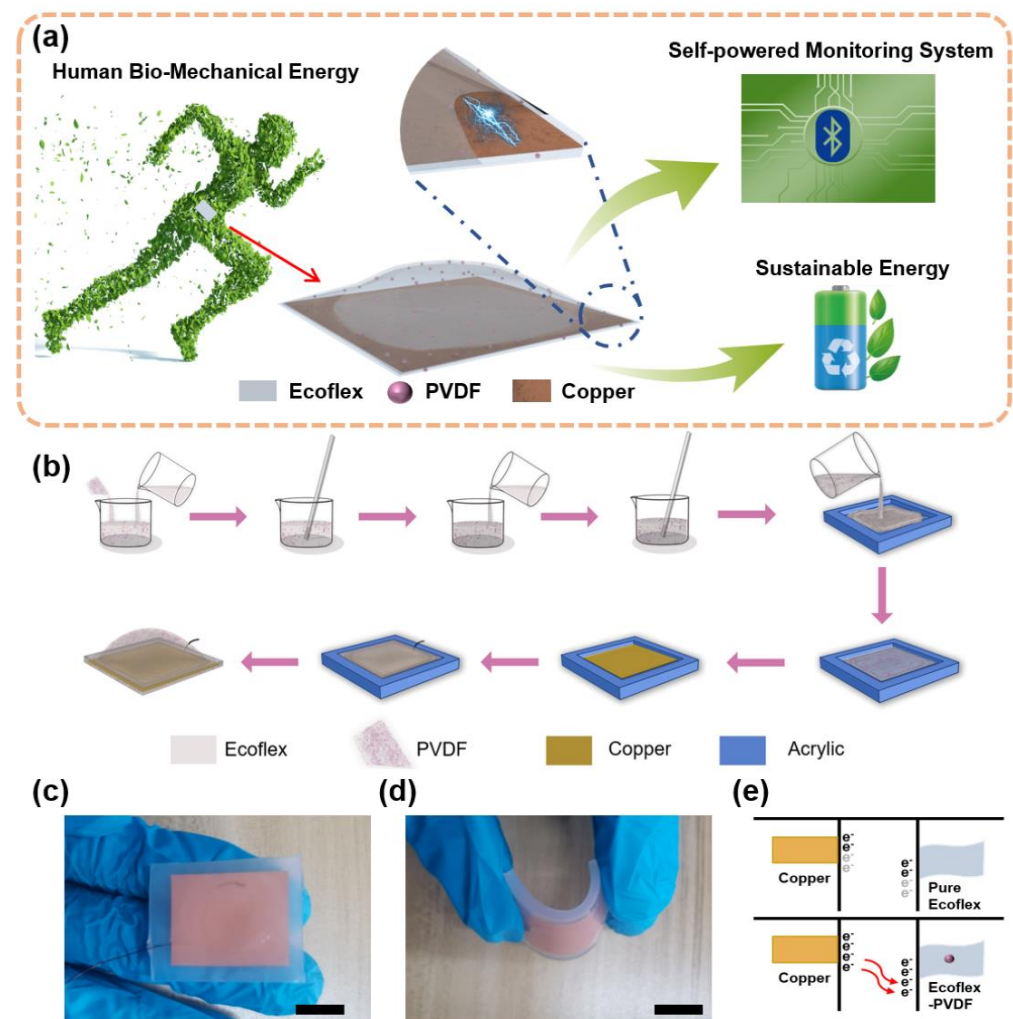


Figure 1. (a) The application schematic illustration of EPGS-TENG for biomechanical energy harvesting and wearable motion monitoring. (b) Schematic illustration of the fabrication of the EPGS-TENG. (c,d) Optical photograph of the EPGS-TENG (c) in the original and (d) bending states. (Scale bars, 1.0 cm.) (e) Schematic of the band diagrams to illustrate the operation mechanism of the proposed EPGS-TENG.

The working principle of the EPGS-TENG is based on the coupling of contact triboelectrification and electrostatic induction [37,38]. In the triboelectric series, silicone rubber and PVDF are triboelectric materials with high electronegativity, while Cu is a triboelectric material with low electronegativity [57]. Specifically, when the distance between the Ecoflex–PVDF composite triboelectric layer and the working electrode is the farthest, the potential difference between the working electrode and the reference electrode (ground) is the largest, as shown in Figure 2a(I). Because silicone rubber has a stronger ability to attract electrons than copper, the surface of the composite triboelectric layer is negatively charged, while the surface of the copper electrode is positively charged. As shown in Figure 2a(II), when the negatively charged silicone rubber layer approaches the copper layer, the potential of the copper electrode decreases, and electrons are driven from the copper layer to the ground. After the upper composite triboelectric layer and the lower copper layer are completely in contact, an equal amount of charges with opposite polarity are generated on the surface, as shown in Figure 2a(III). Contrary to Figure 2a(II), when the composite triboelectric layer leaves the copper layer, the potential of the copper electrode rises, and the electrons will be driven to flow back to the copper electrode from the ground, as shown in Figure 2a(IV). When the contact separation motion is repeated between the composite triboelectric layer and the working electrode, alternating current can be gener-

ated. In order to better understand the working principle of EPGS-TENG quantitatively, COMSOL software was used to simulate the numerical calculation of the space electric field when the composite triboelectric layer and the working electrode are periodically in contact (Figure 2b).

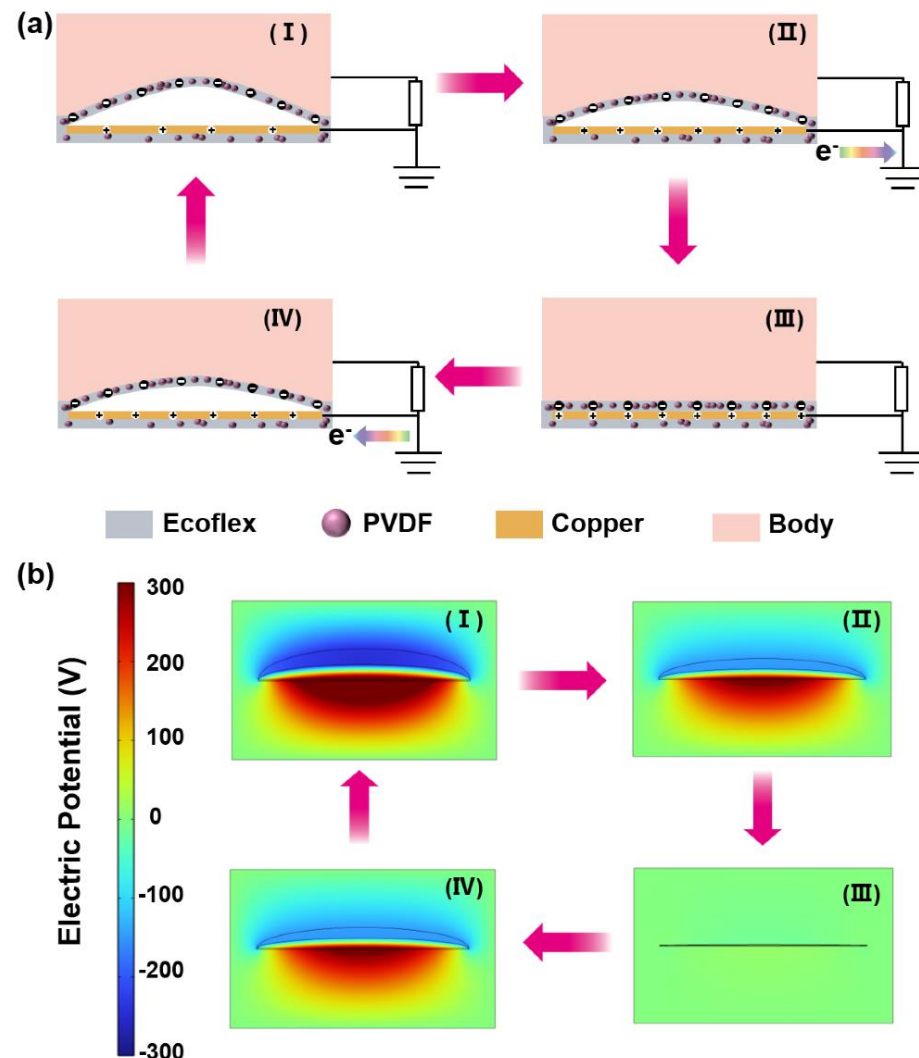


Figure 2. (a) Schematic diagram of the working principle of the EPGS-TENG. (b) FEA simulation of the EPGS-TENG electric potential distribution.

Firstly, we evaluated the influence of different fillers on the voltage output of the device (as shown in Figure 3a). PVDF gives the device the highest voltage output compared to other fillers. Then, we tested the influence of different concentrations (from 0 to 2 wt%) of PVDF in EPGS-PVDF composite on the output voltage of the device under the same equipment and input conditions. As shown in Figure 3b, the output voltage of EPGS-TENG increases with the increase in PVDF filler concentration in the range of 0–1.5 wt%. When the concentration of PVDF is at 1.5 wt%, the maximum peak voltage of EPGS-TENG is 37 V, which is 13 times that of pure Ecoflex. Then, further adding PVDF filler will lead to the voltage of EPGS-TENG dropping. In order to detect the voltage output of the manufactured EPGS-TENG in various states, we systematically tested the EPGS-TENG by using a customized test platform. The test platform is shown in Figure S1. The voltage output of the EPGS-TENG at different pressures and fixed frequencies (1 Hz) is shown in Figure 3c. The results show that the voltage output of EPGS-TENG initially rapidly increases with the increase in pressure, and then has a tendency to flatten. The

relationship between peak voltage and pressure is shown in Figure 3d. Due to the difference in sensitivities, the data in Figure 3d are divided into two linear regions. In region 1 (1 N–10 N), the sensitivity of the EPGS-TENG can reach 7.57 V/N (Slope = $\Delta V/\Delta N$), and the linear fitting data are good ($R^2 = 0.98$). In region 2, the sensitivity of EPGS-TENG is 0.512 V/N, and the variance is 0.69. The results show that EPGS-TENG can monitor external tiny movements. The relationship between output voltage and frequency is shown in Figure 3e. When the input frequency is 0.5 Hz, 1 Hz, 1.5 Hz, 2 Hz, 2.5 Hz, and 3 Hz, the voltage output is 21.8 V, 21.7 V, 21.8 V, 21.8 V, and 21.7 V, respectively. Figure S2 shows the response at different frequencies. The response of the EPGS-TENG can be calculated by the following equation:

$$R\% = \left| \frac{V_0 - V_i}{V_i} \right| \times 100\%, \quad (1)$$

where V_0 and V_i are the output voltage at 0.5 Hz and the output voltage at other frequencies, respectively. When the frequency is 0.5 Hz, 1 Hz, 1.5 Hz, 2 Hz, 2.5 Hz, and 3 Hz under a pressure of 5 N, the response of the EPGS-TENG is 0%, 0.4%, 0%, 0%, 0.2%, and 0.3%, respectively. The results show that the EPGS-TENG has excellent stability under low-frequency motion. Figure 3f shows the voltage output of the EPGS-TENG at different bending angles. When Angle θ is 176°, 170°, 164°, 158°, and 152°, the voltage output is 2.7 V, 4.6 V, 7.2 V, 10.4 V, and 12.8 V, respectively. The response at different bending angles is shown in Figure S3. At different bending angles, the output voltage responses are 0%, 68.9%, 166.7%, 285.2%, and 374.1%. The results show that EPGS-TENG has sensitive angle response ability. Because EPGS-TENG is attached to the human body, we consider the complexity of environmental temperature, and explore the influence of temperature on the output of the device. As shown in Figure 3g and Figure S3, the output voltage of the EPGS-TENG hardly changes when the ambient temperature changes between 20 °C and 40 °C. In practical application, EPGS-TENG must work for a long time, which requires the durability and mechanical stability of the device. In order to solve this problem, we conducted a durability test for 3 h and measured the voltage output of EPGS-TENG. The operating forces and frequencies used in the durability tests were 3 N and 2 Hz, respectively. As shown in Figure 3h, the output voltage of the EPGS-TENG is stable, and there is no significant drop in the whole test period. Detail of the durability test is shown in Figure S6. On the other hand, we collected the output voltage of the EPGS-TENG in its initial state and at room temperature for 10 days. After 10 days of storage, the output voltage of the EPGS-TENG had no obvious change. The above results show that the NSTENG has good reliability and stability while in operation.

Figure 4a shows the changes in output voltage and the calculated current signal of the EPGS-TENG at different load resistors. The results can be obtained by measuring the voltages across different load resistors from 1 to 18 M Ω (the motion conditions applied to EPGS-TENG are 10 N and 2 Hz). It can be observed that the voltage increases and the current decreases with the increase in the load resistance. The output power of EPGS-TENG at different load resistors is shown in Figure 4b. The EPGS-TENG provides a maximum power output of 121 μ W at a resistance of 5 M Ω . Figure 4c and the Movie S2 show the real-time application ability of EPGS-TENG. The 120 series-connected green LEDs can be lit up by tapping the EPGS-TENG by hand. Inspired by the high output performance of the EPGS-TENG, it can be used as a biomechanical energy harvester to power electronic products. The equivalent circuit of the automatic charging system is shown in Figure 4d, whose working circuit consists of EPGS-TENG, a rectifier bridge, a capacitor, a switch, and a load. The alternating current generated by the EPGS-TENG can be converted to direct current through the rectifier bridge. Meanwhile, the electricity generated by the EPGS-TENG can be stored in a capacitor. The switch is used to control the charging and discharging process. Figure 4e shows the charging curves of the 2.2 μ F capacitor by the EPGS-TENG with different motion frequencies. At the frequencies of 1 Hz, 1.5 Hz, 2 Hz, 2.5 Hz, and 3 Hz (room temperature and 15 N pressure), the capacitor of 2.2 μ F can be charged to 1.4 V, 2.2 V, 2.5 V, 3 V, 3.4 V, and 3.4 V, respectively. The results show that the

charging voltage increases with the increase in mobile frequency. Figure 4f shows the voltage–time curves of the EPGS-TENG charging different capacitors. The capacitors of 1 μF , 2.2 μF , 3.3 μF , 4.7 μF , and 10 μF can be charged to 3.8 V, 3.1 V, 2.5 V, 2.1 V, and 1.3 V, respectively, after being charged at room temperature, 15 N pressure, and 3 Hz working frequency for 60 s. The EPGS-TENG can be used as a power source to provide stable and sustainable energy for wearable or portable electronic devices without an external energy supply. As shown in Figure 4g and Movie S3, tapping EPGS-TENG charges 4.7 μF and powers the electronic watch. The tapping frequency is about 2–3 Hz. At about 50 s, the voltage of the capacitor reaches 1.55 V, which can power the watch for about 5 s. Subsequently, the capacitor can be charged back to 1.55 V in about 56–79 s to repeatedly power the watch. Detailed charging and discharging curves are shown in Figure 4h. In addition, Figure 4i and Movie S4 show that the EPGS-TENG can power an electronic calculator. These experimental results confirm that the EPGS-TENG has great potential in a completely self-powered and sustainable electronic system.

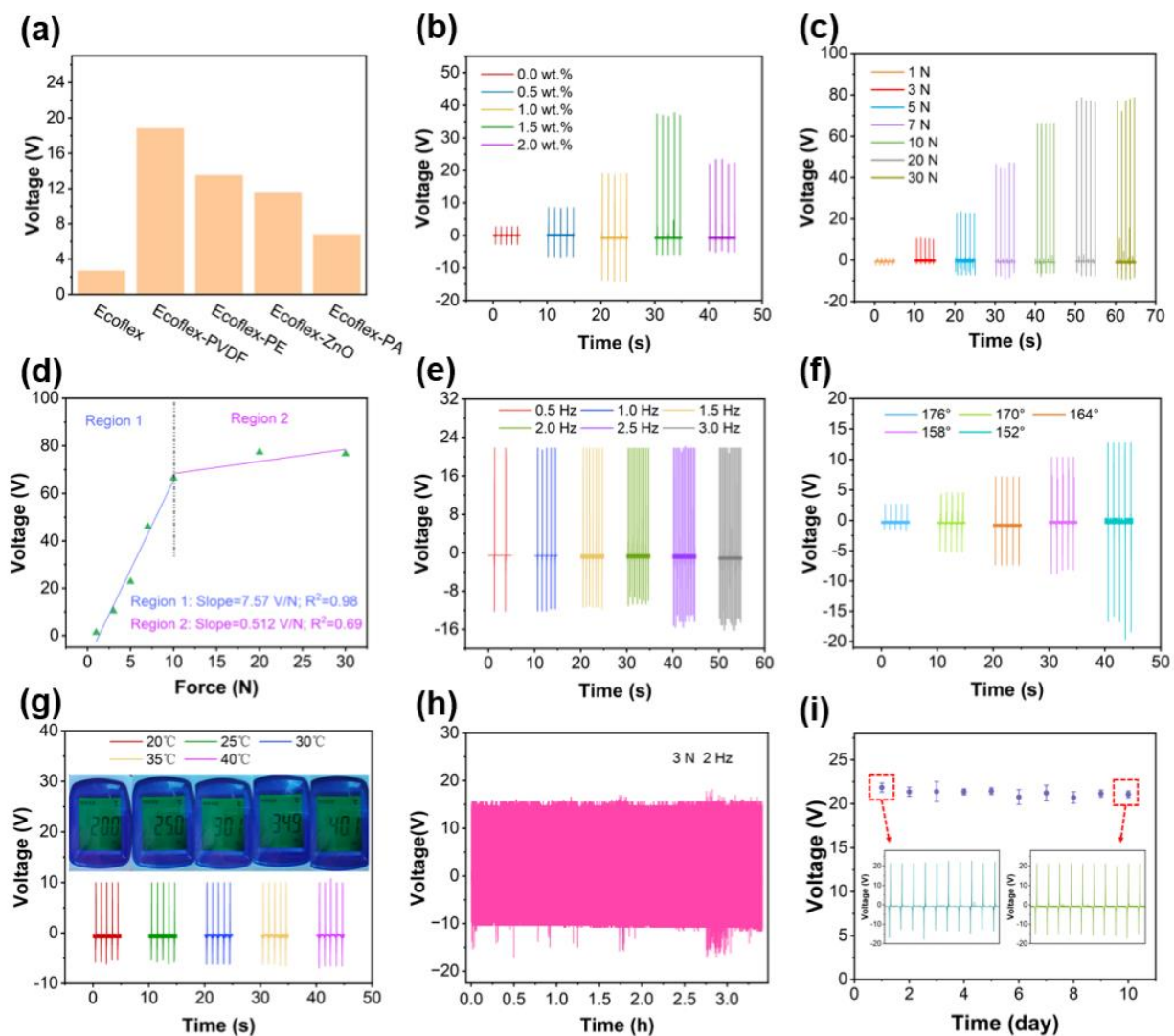


Figure 3. Electrical output characteristics and stability of EPGS-TENG. (a) The influence of different fillers on the electrical output of the device. (b) The output voltage of the EPGS-TENG for various concentrations of PVDF in Ecoflex–PVDF composite under a force of 7 N. (c) The output voltage of the EPGS-TENG under different pressures. (d) The linear fitting analysis of the EPGS-TENG output voltage and pressure. (e–g) The output voltage of the EPGS-Teng at different frequencies, degrees, and temperatures. (h) Durability test of the EPGS-TENG for 3 h. (i) The voltage change of EPGS-TENG within 10 days.

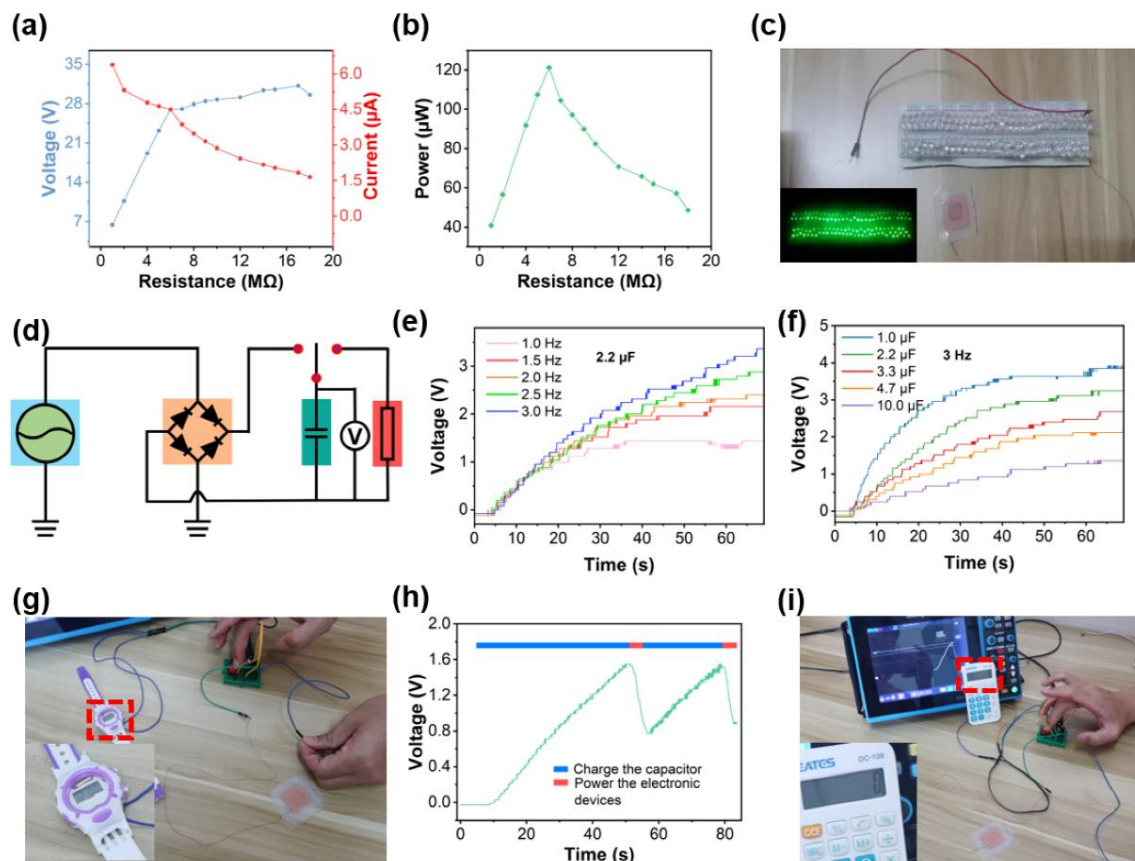


Figure 4. Biomechanical energy harvesting by the EPGS-TENG. (a) Dependence of the output voltage and current at various load resistance. (b) Dependence of the power at various load resistance. (c) Photographs of 120 serially connected LEDs driven by hand tapping. The inset shows the LEDs array with lights on. (d) The equivalent circuit of a self-charging system that uses the energy harvested from the EPGS-TENG to power electronics. (e) Charging voltage of capacitor which is charged by EPGS-TENG on different motion frequencies. (f) Charging voltage of different capacitor which is charged by EPGS-TENG. (g) Powering for an electronic watch. (h) Charging and discharging curve of a capacitor ($4.7 \mu\text{F}$) connected to an electronic watch. (i) Powering for an electronic calculator.

EPGS-TENG can not only be used as a biomechanical energy harvester but can also generate electric signals that directly respond to external mechanical actions. Therefore, the EPGS-TENG can be used as a self-powered sensor to monitor human motion. As shown in Figure 5a, the EPGS-TENG can monitor information such as runners' running posture, and breathing rhythm, and digitize this information to provide a database for sports-related big data. Running for a long time can effectively improve the functions of the digestive system, respiratory system, and other systems, but the wrong running posture will do harm to the body [58–61]. As shown in Figure 5b, the EPGS-TENG can accurately monitor the bending angle of a runner's knee, and the output voltage of EPGS-TENG increases with the increase in the bending angle. These digital data will facilitate runners to understand and control their running posture. The rhythm of the arm swing is very important when running. Runners can control their running speed by controlling their swing arm. As shown in Figure 5c, an EPGS-TENG attached to the inside of the arm can monitor the runner's swing arm rhythm. The output voltage of the slow swing arm will be smaller than that of the fast swing arm, and the time interval between two adjacent peak voltages in the slow swing arm is longer than that of the fast swing arm. Breathing is very important in running because the rhythm of breathing reflects the intensity of running. As shown in Figure 5d, an EPGS-TENG can be attached to the abdomen of runners to monitor their breathing rhythm. During long-distance running, runners should control

their breathing rhythm and actively take deep breaths to meet the oxygen demand of the body. When shortness of breath occurs during running, runners should slow down their running speed to avoid the rapid generation of fatigue. The EPGS-TENG can be placed on the heel to monitor the human movement state, as shown in Figure 5e. In addition, in order to apply EPGS-TENG to practice more conveniently, we have made a wireless transmission system with an EPGS-TENG as a self-powered sensor (Figure 5f). The Bluetooth module of the wireless transmission system is shown in Figure S7. The application of the wireless monitoring system is shown in detail in Figure 5g,h, and in Movies S5 and S6. The above demonstrations show that the EPGS-TENG has a broad application prospects in wearable electronic devices.

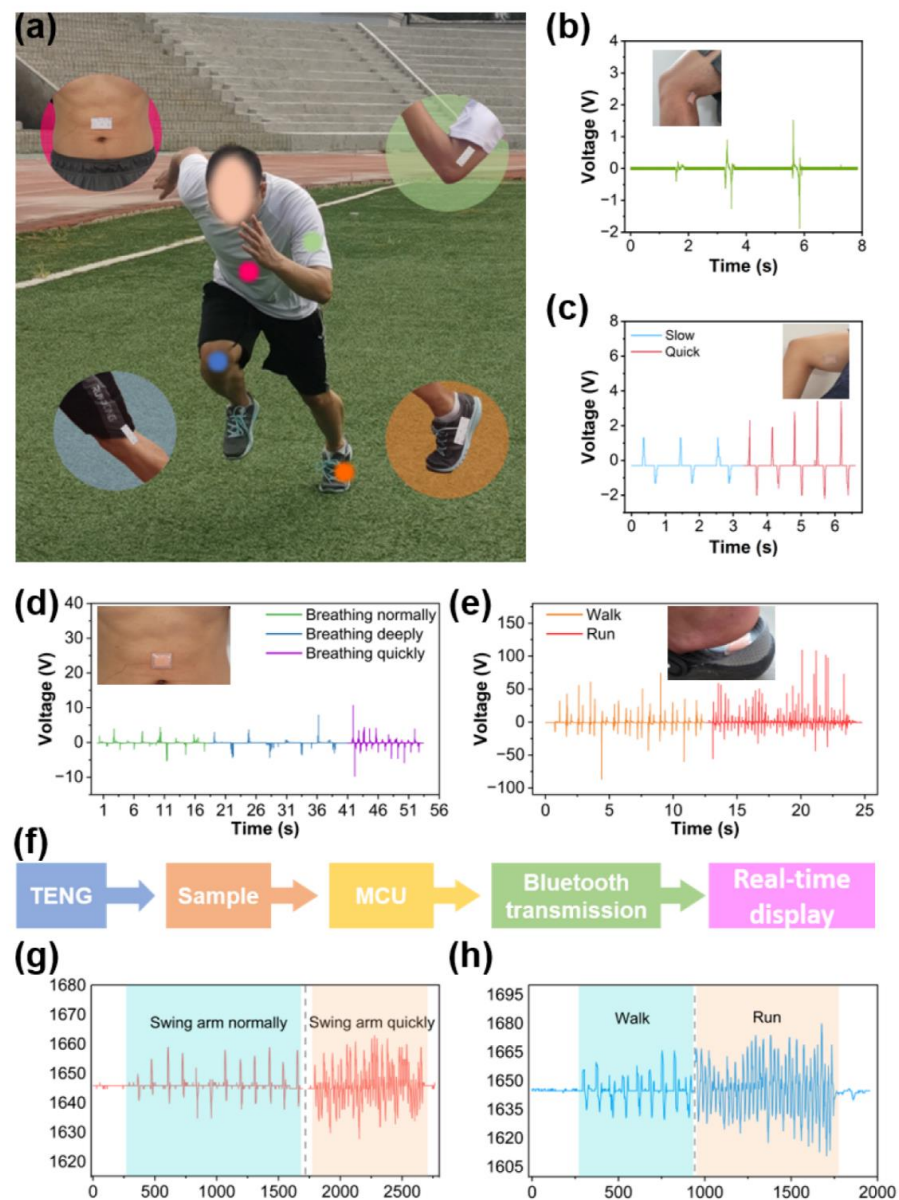


Figure 5. (a) The applications of EPGS-TENG as wearable self-powered sensors for detecting various human motions. The signals output of self-powered sensor attached (b) on a knee joint for monitor leg bending angle, (c) on the inside of an arm to collect swing arm information, (d) on the abdomen to monitor the rate of breathing, and (e) attached at the heel to obtain the walking and running information. (f) Wireless transmission system based on triboelectric nanogenerator. (g) Swing arm information collected by wireless transmission system. (h) Walk and run information collected by wireless transmission system.

4. Conclusions

In summary, we fabricated a gas-supported triboelectric nanogenerator by evaporating soaked deionized water to generate an air gap in situ. Additionally, we added PVDF nanofillers to silicone rubber to improve the performance of the triboelectric nanogenerator. When PVDF is added to the optimal ratio (1.5 wt%), the voltage output of the EPGS-TENG is 13 times that of pure Ecoflex. Then, the output performance and stability of the EPGS-TENG were measured systematically (pressure sensitivity of 7.57 V/N, angle response of 374%, output power of 121 μ W, temperature adaptability from 20 °C to 40 °C, durability over 3 h, and stability of 10 days). The EPGS-TENG exhibits excellent biomechanical energy harvesting capability, and it can continuously drive small electronic devices such as electronic watches and electronic calculators. In addition, the wireless sensor system based on EPGS-TENG can accurately monitor the movement information of the runner. In the future, as a new-generation wearable device, EPGS-TENG will show great potential in the fields of intelligent sports, soft robots, and self-powered biomedical monitoring.

Supplementary Materials: The following supporting information can be downloaded at: <https://www.mdpi.com/article/10.3390/su142114422/s1>, Figure S1: The cross-sectional view of EPGS-TENG, Figure S2: The test platform, Figure S3: The response of output voltage of EPGS-TENG at different frequencies, Figure S4: The response of output voltage of EPGS-TENG at different angles, Figure S5: The response of output voltage of EPGS-TENG at different temperatures, Figure S6: The detail of durability test, Figure S7: The Bluetooth module for wireless transmission system, Movie S1: Demonstration of the gas support structure of the EPGS-TENG, Movie S2: EPGS-TENG lights 120 LEDs, Movie S3: Powering for an electronic watch, Movie S4: Powering for an electronic calculator, Movie S5: Swing arm motion monitoring based on wireless transmission system, Movie S6: Information monitoring of walking and running based on wireless transmission system.

Author Contributions: The manuscript was written through the contributions of all authors. C.J., Q.W., Y.M., and C.Z. conceived the idea; C.J. fabricated the EPGS-TENG; the data were collected, sorted out, and analyzed by Y.Z. and F.S.; Y.W. and Y.L. made the verification and visualization; C.J. and C.Z. wrote the manuscript; Q.W., Y.M., and C.Z. supervised the project. All authors have read and agreed to the published version of the manuscript.

Funding: This research was funded by the planning project of Liaoning Sports Science Association (2022LTXH085, 2022LTXH082), the “Research on the development and application of college sports” of China Higher Education Association (21TYB16), and the education planning project of Liaoning Sports Science Association (LTXKY-2921-021).

Institutional Review Board Statement: Not applicable.

Informed Consent Statement: Not applicable.

Data Availability Statement: The data presented in this study are available in Supplementary Materials.

Acknowledgments: The authors would like to thank the collaboration of all volunteers who participated in data collection.

Conflicts of Interest: The authors declare no conflict of interest.

References

1. Cheng, Y.; Lu, X.; Chan, K.H.; Wang, R.R.; Cao, Z.R.; Sun, J.; Ho, G.W. A stretchable fiber nanogenerator for versatile mechanical energy harvesting and self-powered full-range personal healthcare monitoring. *Nano Energy* **2017**, *41*, 511–518. [[CrossRef](#)]
2. Ouyang, H.; Tian, J.J.; Sun, G.L.; Zou, Y.; Liu, Z.; Li, H.; Zhao, L.M.; Shi, B.J.; Fan, Y.B.; Fan, Y.F.; et al. Self-Powered Pulse Sensor for Antidiastole of Cardiovascular Disease. *Adv. Mater.* **2017**, *29*, 1703456. [[CrossRef](#)]
3. Wang, Y.L.; Zhu, W.; Deng, Y.; Fu, B.; Zhu, P.C.; Yu, Y.D.; Li, J.; Guo, J.J. Self-powered wearable pressure sensing system for continuous healthcare monitoring enabled by flexible thin-film thermoelectric generator. *Nano Energy* **2020**, *73*, 104773. [[CrossRef](#)]
4. Luo, J.J.; Gao, W.C.; Wang, Z.L. The Triboelectric Nanogenerator as an Innovative Technology toward Intelligent Sports. *Adv. Mater.* **2021**, *33*, 2004178. [[CrossRef](#)] [[PubMed](#)]
5. Zhao, T.M.; Fu, Y.M.; Sun, C.X.; Zhao, X.S.; Jiao, C.X.; Du, A.; Wang, Q.; Mao, Y.P.; Liu, B.D. Wearable biosensors for real-time sweat analysis and body motion capture based on stretchable fiber-based triboelectric nanogenerators. *Biosens. Bioelectron.* **2022**, *205*, 114115. [[CrossRef](#)] [[PubMed](#)]

6. Mao, Y.P.; Zhu, Y.S.; Zhao, T.M.; Jia, C.J.; Bian, M.Y.; Li, X.X.; Liu, Y.G.; Liu, B.D. A Portable and Flexible Self-Powered Multifunctional Sensor for Real-Time Monitoring in Swimming. *Biosensors* **2021**, *11*, 147. [[CrossRef](#)]
7. Dong, K.; Peng, X.; An, J.; Wang, A.C.; Luo, J.J.; Sun, B.Z.; Wang, J.; Wang, Z.L. Shape adaptable and highly resilient 3D braided triboelectric nanogenerators as e-textiles for power and sensing. *Nat. Commun.* **2020**, *11*, 2868. [[CrossRef](#)]
8. Chen, C.Y.; Chen, L.J.; Wu, Z.Y.; Guo, H.Y.; Yu, W.D.; Du, Z.Q.; Wang, Z.L. 3D double-faced interlock fabric triboelectric nanogenerator for bio-motion energy harvesting and as self-powered stretching and 3D tactile sensors. *Mater. Today* **2020**, *32*, 84–93. [[CrossRef](#)]
9. Yan, Z.G.; Wang, L.L.; Xia, Y.F.; Qiu, R.D.; Liu, W.Q.; Wu, M.; Zhu, Y.; Zhu, S.L.; Jia, C.Y.; Zhu, M.M.; et al. Flexible High-Resolution Triboelectric Sensor Array Based on Patterned Laser-Induced Graphene for Self-Powered Real-Time Tactile Sensing. *Adv. Funct. Mater.* **2021**, *31*, 2100709. [[CrossRef](#)]
10. Cao, X.; Jie, Y.; Wang, N.; Wang, Z.L. Triboelectric Nanogenerators Driven Self-Powered Electrochemical Processes for Energy and Environmental Science. *Adv. Energy Mater.* **2016**, *6*, 1600665. [[CrossRef](#)]
11. Vikhareva, I.N.; Aminova, G.K.; Mazitova, A.K. Resource Cycling: Application of Anaerobic Utilization Methods. *Sustainability* **2022**, *14*, 9278. [[CrossRef](#)]
12. Niu, L.; Peng, X.; Chen, L.J.; Liu, Q.; Wang, T.R.; Dong, K.; Pan, H.; Cong, H.L.; Liu, G.L.; Jiang, G.M.; et al. Industrial production of bionic scales knitting fabric-based triboelectric nanogenerator for outdoor rescue and human protection. *Nano Energy* **2022**, *97*, 107168. [[CrossRef](#)]
13. Li, M.; Yang, Y.G.; Wang, Z.K.; Kang, T.; Wang, Q.; Turren-Cruz, S.H.; Gao, X.Y.; Hsu, C.S.; Liao, L.S.; Abate, A. Perovskite Grains Embraced in a Soft Fullerene Network Make Highly Efficient Flexible Solar Cells with Superior Mechanical Stability. *Adv. Mater.* **2019**, *31*, 1901519. [[CrossRef](#)]
14. Elomari, Y.; Norouzi, M.; Marin-Genesca, M.; Fernandez, A.; Boer, D. Integration of Solar Photovoltaic Systems into Power Networks: A Scientific Evolution Analysis. *Sustainability* **2022**, *14*, 9249. [[CrossRef](#)]
15. Burmistrov, I.; Khanna, R.; Gorshkov, N.; Kiselev, N.; Artyukhov, D.; Boychenko, E.; Yudin, A.; Konyukhov, Y.; Kravchenko, M.; Gorokhovskiy, A.; et al. Advances in Thermo-Electrochemical (TEC) Cell Performances for Harvesting Low-Grade Heat Energy: A Review. *Sustainability* **2022**, *14*, 9483. [[CrossRef](#)]
16. Jaziri, N.; Boughamoura, A.; Muller, J.; Mezghani, B.; Tounsi, F.; Ismail, M. A comprehensive review of Thermoelectric Generators: Technologies and common applications. *Energy Rep.* **2020**, *6*, 264–287. [[CrossRef](#)]
17. Park, D.Y.; Joe, D.J.; Kim, D.H.; Park, H.; Han, J.H.; Jeong, C.K.; Park, H.; Park, J.G.; Joung, B.; Lee, K.J. Self-Powered Real-Time Arterial Pulse Monitoring Using Ultrathin Epidermal Piezoelectric Sensors. *Adv. Mater.* **2017**, *29*, 1702308. [[CrossRef](#)]
18. Moorthy, B.; Baek, C.; Wang, J.E.; Jeong, C.K.; Moon, S.; Park, K.I.; Kim, D.K. Piezoelectric energy harvesting from a PMN-PT single nanowire. *RSC Adv.* **2017**, *7*, 260–265. [[CrossRef](#)]
19. Yang, W.Q.; Chen, J.; Zhu, G.; Wen, X.N.; Bai, P.; Su, Y.J.; Lin, Y.; Wang, Z.L. Harvesting vibration energy by a triple-cantilever based triboelectric nanogenerator. *Nano Res.* **2013**, *6*, 880–886. [[CrossRef](#)]
20. Liu, Y.K.; Liu, W.L.; Wang, Z.; He, W.C.; Tang, Q.; Xi, Y.; Wang, X.; Guo, H.Y.; Hu, C.G. Quantifying contact status and the air-breakdown model of charge-excitation triboelectric nanogenerators to maximize charge density. *Nat. Commun.* **2020**, *11*, 1599. [[CrossRef](#)]
21. Wang, J.; Wu, C.S.; Dai, Y.J.; Zhao, Z.H.; Wang, A.; Zhang, T.J.; Wang, Z.L. Achieving ultrahigh triboelectric charge density for efficient energy harvesting. *Nat. Commun.* **2017**, *8*, 88. [[CrossRef](#)] [[PubMed](#)]
22. Liu, W.L.; Wang, Z.; Wang, G.; Zeng, Q.X.; He, W.C.; Liu, L.Y.; Wang, X.; Xi, Y.; Guo, H.Y.; Hu, C.G.; et al. Switched-capacitor-converters based on fractal design for output power management of triboelectric nanogenerator. *Nat. Commun.* **2020**, *11*, 1883. [[CrossRef](#)] [[PubMed](#)]
23. Sun, F.X.; Zhu, Y.S.; Jia, C.J.; Ouyang, B.W.; Zhao, T.M.; Li, C.X.; Ba, N.; Li, X.; Chen, S.; Che, T.T.; et al. A Flexible Lightweight Triboelectric Nanogenerator for Protector and Scoring System in Taekwondo Competition Monitoring. *Electronics* **2022**, *11*, 1306. [[CrossRef](#)]
24. Lin, H.B.; Liu, Y.; Chen, S.L.; Xu, Q.H.; Wang, S.T.; Hu, T.; Pan, P.F.; Wang, Y.Z.; Zhang, Y.L.; Li, N.; et al. Seesaw structured triboelectric nanogenerator with enhanced output performance and its applications in self-powered motion sensing. *Nano Energy* **2019**, *65*, 103944. [[CrossRef](#)]
25. Zhang, J.H.; Xu, Q.H.; Li, H.; Zhang, S.Y.; Jiang, Y.W.; Hu, N.; Chen, G.L.; Fu, H.Y.; Yuan, M.; Dai, B.Y.; et al. Self-Powered Electrodeposition System for Sub-10-nm Silver Nanoparticles with High-Efficiency Antibacterial Activity. *J. Phys. Chem. Lett.* **2022**, *13*, 6721–6730. [[CrossRef](#)]
26. Guo, H.Y.; Chen, J.; Yeh, M.H.; Fan, X.; Wen, Z.; Li, Z.L.; Hu, C.G.; Wang, Z.L. An Ultrarobust High-Performance Triboelectric Nanogenerator Based on Charge Replenishment. *ACS Nano* **2015**, *9*, 5577–5584. [[CrossRef](#)]
27. Chen, J.; Ren, Y.C.; Xiang, H.Y.; Jiang, X.P.; Yang, X.H.; Guo, H.Y. A self-powered human-pet interaction system enabled by triboelectric nanogenerator functionalized pet-leash. *Nano Energy* **2022**, *101*, 107597. [[CrossRef](#)]
28. Guo, H.Y.; Pu, X.J.; Chen, J.; Meng, Y.; Yeh, M.H.; Liu, G.L.; Tang, Q.; Chen, B.D.; Liu, D.; Qi, S.; et al. A highly sensitive, self-powered triboelectric auditory sensor for social robotics and hearing aids. *Sci. Robot* **2018**, *3*, eaat2516. [[CrossRef](#)]
29. He, W.C.; Liu, W.L.; Fu, S.K.; Wu, H.Y.; Shan, C.C.; Wang, Z.; Xi, Y.; Wang, X.; Guo, H.Y.; Liu, H.; et al. Ultrahigh Performance Triboelectric Nanogenerator Enabled by Charge Transmission in Interfacial Lubrication and Potential Decentralization Design. *Research* **2022**, *2022*, 9812865. [[CrossRef](#)]

30. Li, G.; Fu, S.K.; Luo, C.Y.; Wang, P.; Du, Y.; Tang, Y.T.; Wang, Z.; He, W.C.; Liu, W.L.; Guo, H.Y.; et al. Constructing high output performance triboelectric nanogenerator via V-shape stack and self-charge excitation. *Nano Energy* **2022**, *96*, 107068. [[CrossRef](#)]
31. Xu, Q.H.; Fang, Y.S.; Jing, B.Q.S.; Hu, N.; Lin, K.; Pan, Y.F.; Xu, L.; Gao, H.Q.; Yuan, M.; Chu, L.; et al. A portable triboelectric spirometer for wireless pulmonary function monitoring. *Biosens. Bioelectron.* **2021**, *187*, 113329. [[CrossRef](#)]
32. Xu, Q.H.; Lu, Y.T.; Zhao, S.Y.; Hu, N.; Jiang, Y.W.; Li, H.; Wang, Y.; Gao, H.Q.; Li, Y.; Yuan, M.; et al. A wind vector detecting system based on triboelectric and photoelectric sensors for simultaneously monitoring wind speed and direction. *Nano Energy* **2021**, *89*, 106382. [[CrossRef](#)]
33. Wang, H.; Cheng, J.; Wang, Z.Z.; Ji, L.H.; Wang, Z.L. Triboelectric nanogenerators for human-health care. *Sci. Bull.* **2021**, *66*, 490–511. [[CrossRef](#)]
34. Mao, Y.P.; Zhu, Y.S.; Zhao, T.M.; Jia, C.J.; Wang, X.; Wang, Q. Portable Mobile Gait Monitor System Based on Triboelectric Nanogenerator for Monitoring Gait and Powering Electronics. *Energies* **2021**, *14*, 4996. [[CrossRef](#)]
35. Yu, J.B.; Hou, X.J.; He, J.; Cui, M.; Wang, C.; Geng, W.P.; Mu, J.L.; Han, B.; Chou, X.J. Ultra-flexible and high-sensitive triboelectric nanogenerator as electronic skin for self-powered human physiological signal monitoring. *Nano Energy* **2020**, *69*, 104437. [[CrossRef](#)]
36. Lu, X.; Zheng, L.; Zhang, H.D.; Wang, W.H.; Wang, Z.L.; Sun, C.W. Stretchable, transparent triboelectric nanogenerator as a highly sensitive self-powered sensor for driver fatigue and distraction monitoring. *Nano Energy* **2020**, *78*, 105359. [[CrossRef](#)]
37. Shao, J.J.; Jiang, T.; Wang, Z.L. Theoretical foundations of triboelectric nanogenerators (TENGs). *Sci. China Technol. Sci.* **2020**, *63*, 1087–1109. [[CrossRef](#)]
38. Wen, X.N.; Su, Y.J.; Yang, Y.; Zhang, H.L.; Wang, Z.L. Applicability of triboelectric generator over a wide range of temperature. *Nano Energy* **2014**, *4*, 150–156. [[CrossRef](#)]
39. Lai, Y.C.; Wu, H.M.; Lin, H.C.; Chang, C.L.; Chou, H.H.; Hsiao, Y.C.; Wu, Y.C. Entirely, Intrinsically, and Autonomously Self-Healable, Highly Transparent, and Superstretchable Triboelectric Nanogenerator for Personal Power Sources and Self-Powered Electronic Skins. *Adv. Funct. Mater.* **2019**, *29*, 1904626. [[CrossRef](#)]
40. Zhao, L.M.; Zheng, Q.; Ouyang, H.; Li, H.; Yan, L.; Shi, B.J.; Li, Z. A size-unlimited surface microstructure modification method for achieving high performance triboelectric nanogenerator. *Nano Energy* **2016**, *28*, 172–178. [[CrossRef](#)]
41. Zhu, Y.S.; Sun, F.X.; Jia, C.J.; Zhao, T.M.; Mao, Y.P. A Stretchable and Self-Healing Hybrid Nano-Generator for Human Motion Monitoring. *Nanomaterials* **2022**, *12*, 104. [[CrossRef](#)] [[PubMed](#)]
42. Mao, Y.P.; Sun, F.X.; Zhu, Y.S.; Jia, C.J.; Zhao, T.M.; Huang, C.R.; Li, C.X.; Ba, N.; Che, T.T.; Chen, S. Nanogenerator-Based Wireless Intelligent Motion Correction System for Storing Mechanical Energy of Human Motion. *Sustainability* **2022**, *14*, 6944. [[CrossRef](#)]
43. Zhao, X.; Zhang, D.; Xu, S.W.; Qian, W.Q.; Han, W.; Wang, Z.L.; Yang, Y. Stretching-enhanced triboelectric nanogenerator for efficient wind energy scavenging and ultrasensitive strain sensing. *Nano Energy* **2020**, *75*, 104920. [[CrossRef](#)]
44. Ni, G.L.; Zhu, X.S.; Mi, H.Y.; Feng, P.Y.; Li, J.; Jing, X.; Dong, B.B.; Liu, C.T.; Shen, C.Y. Skinless porous films generated by supercritical CO₂ foaming for high-performance complementary shaped triboelectric nanogenerators and self-powered sensors. *Nano Energy* **2021**, *87*, 106148. [[CrossRef](#)]
45. Kim, D.W.; Lee, J.H.; You, I.; Kim, J.K.; Jeong, U. Adding a stretchable deep-trap interlayer for high-performance stretchable triboelectric nanogenerators. *Nano Energy* **2018**, *50*, 192–200. [[CrossRef](#)]
46. Rahman, M.T.; Rana, S.M.S.; Abu Zahed, M.; Lee, S.; Yoon, E.S.; Park, J.Y. Metal-organic framework-derived nanoporous carbon incorporated nanofibers for high-performance triboelectric nanogenerators and self-powered sensors. *Nano Energy* **2022**, *94*, 106921. [[CrossRef](#)]
47. Yang, W.; Chen, H.M.; Wu, M.Q.; Sun, Z.Y.; Gao, M.; Li, W.J.; Li, C.Y.; Yu, H.L.; Zhang, C.; Xu, Y.; et al. A Flexible Triboelectric Nanogenerator Based on Cellulose-Reinforced MXene Composite Film. *Adv. Mater. Interfaces* **2022**, *9*, 2102124. [[CrossRef](#)]
48. Zhao, D.N.; Zhuo, J.T.; Chen, Z.T.; Wu, J.J.; Ma, R.; Zhang, X.J.; Zhang, Y.F.; Wang, X.; Wei, X.S.; Liu, L.X.; et al. Eco-friendly in-situ gap generation of no-spacer triboelectric nanogenerator for monitoring cardiovascular activities. *Nano Energy* **2021**, *90*, 106580. [[CrossRef](#)]
49. Guo, Z.H.; Wang, H.L.; Shao, J.J.; Shao, Y.S.; Jia, L.Y.; Li, L.W.; Pu, X.; Wang, Z.L. Bioinspired soft electroreceptors for artificial precontact somatosensation. *Sci. Adv.* **2022**, *8*, eabo5201. [[CrossRef](#)]
50. Han, K.; Luo, J.J.; Chen, J.; Chen, B.D.; Xu, L.; Feng, Y.W.; Tang, W.; Wang, Z.L. Self-powered ammonia synthesis under ambient conditions via N₂ discharge driven by Tesla turbine triboelectric nanogenerators. *Microsyst. Nanoeng.* **2021**, *7*, 7. [[CrossRef](#)]
51. Du, S.; Suo, H.N.; Xie, G.; Lyu, Q.Q.; Mo, M.; Xie, Z.J.; Zhou, N.Y.; Zhang, L.B.; Tao, J.; Zhu, J.T. Self-powered and photothermal electronic skin patches for accelerating wound healing. *Nano Energy* **2022**, *93*, 106906. [[CrossRef](#)]
52. Shrestha, K.; Sharma, S.; Pradhan, G.B.; Bhatta, T.; Maharjan, P.; Rana, S.S.; Lee, S.; Seonu, S.; Shin, Y.; Park, J.Y. A Siloxene/Ecoflex Nanocomposite-Based Triboelectric Nanogenerator with Enhanced Charge Retention by MoS₂/LIG for Self-Powered Touchless Sensor Applications. *Adv. Funct. Mater.* **2022**, *32*, 2113005. [[CrossRef](#)]
53. Liu, X.; Sun, X.R.; Luo, C.; Ma, H.Z.; Yu, H.; Shao, Y.; Yang, M.B.; Yin, B. Improvement in the output performance of polyethylene oxide-based triboelectric nanogenerators by introducing core-shell Ag@SiO₂ particles. *J. Mater. Chem. C* **2021**, *10*, 265–273. [[CrossRef](#)]
54. Luo, X.X.; Liu, L.D.; Wang, Y.C.; Li, J.Y.; Berbille, A.; Zhu, L.P.; Wang, Z.L. Tribovoltaic Nanogenerators Based on MXene-Silicon Heterojunctions for Highly Stable Self-Powered Speed, Displacement, Tension, Oscillation Angle, and Vibration Sensors. *Adv. Funct. Mater.* **2022**, *32*, 2113149. [[CrossRef](#)]

55. Wang, J.J.; Cui, P.; Zhang, J.J.; Ge, Y.; Liu, X.L.; Xuan, N.N.; Gu, G.Q.; Cheng, G.; Du, Z.L. A stretchable self-powered triboelectric tactile sensor with EGaIn alloy electrode for ultra-low-pressure detection. *Nano Energy* **2021**, *89*, 106320. [[CrossRef](#)]
56. Fan, B.B.; Liu, G.X.; Fu, X.P.; Wang, Z.Z.; Zhang, Z.; Zhang, C. Composite film with hollow hierarchical silica/perfluoropolyether filler and surface etching for performance enhanced triboelectric nanogenerators. *Chem. Eng. J.* **2022**, *446*, 137263. [[CrossRef](#)]
57. Zou, H.Y.; Zhang, Y.; Guo, L.T.; Wang, P.H.; He, X.; Dai, G.Z.; Zheng, H.W.; Chen, C.Y.; Wang, A.C.; Xu, C.; et al. Quantifying the triboelectric series. *Nat. Commun.* **2019**, *10*, 1427. [[CrossRef](#)]
58. Podvigina, T.T.; Yarushkina, N.I.; Filaretova, L.P. Effects of Running on the Development of Diabetes and Diabetes-Induced Complications. *J. Evol. Biochem. Phys.* **2022**, *58*, 174–192. [[CrossRef](#)]
59. Spaulding, H.; Selsby, J. Is Exercise the Right Medicine for Dystrophic Muscle? *Med. Sci. Sports Exerc.* **2018**, *50*, 1723–1732. [[CrossRef](#)]
60. Skof, B.; Milic, R. The Effect of a Six-Month Training Programme on the Endurance and Aerobic Capacity Parameters of Adult Women. *Zdrav. Varst.* **2010**, *49*, 124–131.
61. Cooper, C.; Moon, H.Y.; van Praag, H. On the Run for Hippocampal Plasticity. *Cold Spring Harb. Perspect. Med.* **2018**, *8*, a029736. [[CrossRef](#)] [[PubMed](#)]